JCB Article

The relationship between force and focal complex development

Catherine G. Galbraith,[1,2] Kenneth M. Yamada,[2] and Michael P. Sheetz[1,3]

[1]Duke University Medical Center, Durham, NC 27710
[2]National Institute of Dental and Craniofacial Research, National Institutes of Health, Bethesda, MD 20892
[3]Department of Biological Sciences, Columbia University, New York, NY 10027

To adhere and migrate, cells must be capable of applying cytoskeletal force to the extracellular matrix (ECM) through integrin receptors. However, it is unclear if connections between integrins and the ECM are immediately capable of transducing cytoskeletal contraction into migration force, or whether engagement of force transmission requires maturation of the adhesion. Here, we show that initial integrin–ECM adhesions become capable of exerting migration force with the recruitment of vinculin, a marker for focal complexes, which are precursors of focal adhesions. We are able to induce the development of focal complexes by the application of mechanical force to fibronectin receptors from inside or outside the cell, and we are able to extend focal complex formation to vitronectin receptors by the removal of c-Src. These results indicate that cells use mechanical force as a signal to strengthen initial integrin–ECM adhesions into focal complexes and regulate the amount of migration force applied to individual adhesions at localized regions of the advancing lamella.

Introduction

The ability of cells to apply cytoskeletal force to the ECM through integrin receptors is critical for migration, embryogenesis, and metastasis. At the front of the cell, new integrin–ECM connections are created and used as sites for the application of migration force (Lauffenburger and Horwitz, 1996; Sheetz et al., 1998). At the rear of the cell, connections are weakened to allow the cell body to move forward (Lauffenburger and Horwitz, 1996; Sheetz et al., 1998). In the middle of the cell, migration forces change direction (Galbraith and Sheetz, 1997), and contractile forces are applied to well-established connections or focal adhesions in order to maintain cell contact with the ECM (Sastry and Burridge, 2000). These regional variations indicate that cells must regulate the size and the amount of force applied to adhesive contacts in order to migrate. Yet, direct measurements comparing the composition or size of adhesive contacts with the amount of migration force applied at the contacts have not identified a clear relationship. If the adhesive contact is $>1\ \mu m^2$, then the size of the adhesion correlates with the amount of force (Lee et al., 1994; Balaban et al., 2001). However, it has also been reported that larger forces are supported at small nascent adhesions, and force decreases as the adhesions mature and increase in size (Pelham and Wang, 1999; Beningo et al., 2001). Thus, it is unclear if adhesions are immediately capable of transducing cytoskeletal contraction into migration force or whether force transmission requires maturation of the adhesion. To address this apparent discrepancy, we applied force to initial connections between integrin receptors and ECM ligands while simultaneously measuring their degree of maturation and ability to exert migration force.

Initial adhesions are formed between integrin receptors and the ECM at the leading edge of migratory cells. These initial adhesions contain actin and talin, and they mature into small focal complexes ($<1\ \mu m^2$ in area) away from the leading edge at the border between the lamellipodia and the lamella (Izzard, 1988) within 60–90 s. The development of the initial adhesion into a focal complex is marked by the recruitment of vinculin (DePasquale and Izzard, 1987; Izzard, 1988), a regulator of cell migration and adhesion (Xu et al., 1998). As vinculin is recruited and the focal complex is formed, there is a decrease in the distance between the adhesion and the ECM-coated surface to form a "tight" or "focal" junction as measured by interference reflection microscopy (DePasquale and Izzard, 1987; Izzard, 1988). The newly formed focal complexes are Rac-dependent structures (Nobes and Hall, 1995) that are tightly adhered to the ECM (DePasquale and Izzard, 1987; Izzard, 1988) and contain all

Address correspondence to Michael P. Sheetz, Dept. of Biological Sciences, Columbia University, PO Box 2408, Sherman Fairchild Center, Rm. 713, 1212 Amsterdam Ave., New York, NY 10027. Tel.: (212) 854-4857. Fax: (212) 854-6399. E-mail: ms2001@columbia.edu

Key words: focal adhesion; vinculin; laser tweezers; migration; force-dependent signaling

of the components of initial adhesions as well as vinculin, paxillin, and phosphoproteins (Nobes and Hall, 1995). Focal complexes can continue to develop into relatively large, stable focal adhesions, extending further from the cell periphery through a Rho-dependent mechanism (Riveline et al., 2001). Focal adhesions contain the subset of proteins that mark focal complexes as well as many others (Geiger and Bershadsky, 2001; Geiger et al., 2001). In addition to containing more molecular components than focal complexes, focal adhesions require much more time (~60 min) to become fully established (Zamir et al., 2000). Because only 3–5 min is required for a cell's migration force to change from a maximum to a minimum force (Galbraith and Sheetz, 1997), which is the same amount of time required to form a focal complex, focal complexes are likely to be important in dynamic migration events. Therefore, we examined whether initial adhesions must mature into focal complexes in order to exert migration force on the ECM.

Because initial integrin–ECM connections (Choquet et al., 1997) and focal complexes (Riveline et al., 2001) are responsive to mechanical stimuli, we probed the relationship between the maturation of an initial adhesion into a focal complex and its ability to exert migration force using two different types of mechanical stimuli. First, we challenged the lamella of motile fibroblasts with different-sized beads coated with a fragment of fibronectin type III, domains 7–10 ($FN_{7–10}$).* We designed the experiments to use a fibronectin fragment containing the cell-binding domain and the synergy site because this type of fragment is incapable of supporting focal adhesions (Fig. 1; Izzard et al., 1986; Woods et al., 1986; Bloom et al., 1999), and they do not stimulate Rho activation (Saoncella et al., 1999). Only the larger $FN_{7–10}$-coated surface elicited Rac-dependent focal complex assembly as a type of "inside-to-outside" signal (Vuori and Ruoslahti, 1999). Second, we developed a new optical laser trap (laser tweezers) assay that allowed monitoring of the force on the beads while visualizing fluorescent protein localization. Tweezer-generated mechanical force was a type of "outside-to-inside" signal, and restrained $FN_{7–10}$-coated beads showed focal complex formation by GFP-vinculin localization. Thus, we were able to use mechanical force to modify initial integrin–ECM connections while measuring the amount of cytoskeletal force exerted on the connection as it matured. Our results demonstrate that force induces the accumulation of the focal complex marker vinculin, which is recruited to initial β1 integrin–$FN_{7–10}$ connections when the connections can exert migration force. Vinculin can also accumulate at vitronectin (VN) receptor sites when they can exert force that occurs in the absence of c-Src. Moreover, we establish that the focal complexes formed at the leading edge of a motile cell exert forces that are smaller than the larger forces exerted by focal adhesions, and these forces do not decrease as the complex enlarges and travels rearward on the lamella. These results indicate that cells use mechanical force as a signal to strengthen initial integrin–ECM adhesions into focal complexes and to dynamically regulate the amount of migration force applied at individual adhesions located along the advancing margin.

*Abbreviations used in this paper: DIC, differential interference contrast; FN, fibronectin; FN_{7-10}, fibronectin type III, domains 7–10; VN, vitronectin.

Results

Internal force induces focal complex formation

To determine whether the area of contact with a ligand-coated surface could influence the type of adhesive complex formed, we added different sizes of ligand-coated beads to the lamella of fibroblasts and examined the pattern of accumulation of vinculin around the beads. We chose vinculin to distinguish between the initial adhesions, focal complexes, and focal adhesions. Vinculin is a marker for focal complexes and focal adhesions that, unlike the focal complex marker talin, is absent from initial adhesions (DePasquale and Izzard, 1987; Izzard, 1988), and unlike the focal complex marker paxillin, has a defined temporal relationship between its accumulation and focal complex formation (DePasquale and Izzard, 1987; Izzard, 1988). Additionally, the ability of vinculin-containing focal complexes (Riveline et al., 2001) and focal adhesions (Galbraith et al., 1998) to elongate in response to force, as well as the correlation between the size of large vinculin aggregates with the amount

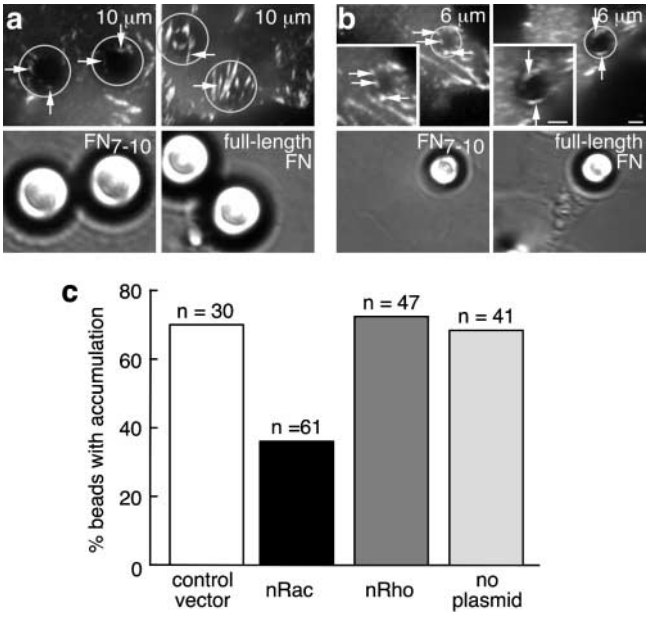

Figure 1. **$FN_{7–10}$-coated beads induce the formation of focal complexes that are inhibited by expression of dominant-negative Rac.** (a) The pattern of vinculin accumulation around large, 10-μm-diam $FN_{7–10}$-coated beads indicates the formation of small punctate focal complexes, whereas vinculin accumulation around full-length FN-coated beads indicates the formation of large focal adhesions. Note that focal planes of the images were chosen to make the vinculin-containing adhesions most visible. Arrows mark adhesions. (b) Focal complexes also form around midsized (6-μm) $FN_{7–10}$-coated beads, whereas focal adhesions form around the same size full-length FN-coated beads. Insets are higher magnification views of regions around the bead. Bars, 2 μm. (c) The focal complexes formed around 6-μm $FN_{7–10}$-coated beads are inhibited by expression of dominant-negative Rac ($P < 0.005$). Expression of dominant-negative Rho or a vector control containing the same promoter did not affect the percentage of beads exhibiting vinculin accumulation. Numbers indicate number of beads scored.

of force generated at stable focal adhesions in stationary cells (Balaban et al., 2001), suggests that vinculin is an indicator of the ability of cells to exert force at adhesive contacts.

Because we wished to follow focal complex formation, we analyzed vinculin accumulation in fibroblast lamellae at beads coated with the cell-binding fragment of fibronectin for 1 h. Large (10-μm diam) fibronectin (FN)-coated beads have been shown to induce the formation of focal adhesions (Fig. 1 a; Grinnell and Geiger, 1986; Miyamoto et al., 1995). However, when large beads were coated with $FN_{7–10}$, which does not contain the domains for supporting focal adhesions (Izzard et al., 1986; Woods et al., 1986; Bloom et al., 1999; unpublished data) or stimulating Rho activation (Saoncella et al., 1999), only small punctate vinculin accumulations that are diagnostic of focal complexes were formed (Fig. 1 a). Similar results were obtained with midsized (6 μm) FN- and $FN_{7–10}$-coated beads (Fig. 1 b). Control experiments demonstrated that the beads were not internalized at 1 h and that there was significant vinculin accumulation around $FN_{7–10}$-coated beads within 20 min (see Materials and methods). These data indicate that $FN_{7–10}$-coated beads induce focal complex formation.

To confirm that we were inducing focal complexes, we examined the dependence of the punctate vinculin accumulation at $FN_{7–10}$-coated beads on the Rho family GTPase Rac, which induces focal complexes (Nobes and Hall, 1995; Rottner et al., 1999). Two different aspects of Rac function support this relationship. First, experimentally induced focal complexes were only observed on the cell lamella, where high GTPase Rac activity has been previously reported (Kraynov et al., 2000). Moreover, the number of vinculin-containing focal complexes produced by 6-μm $FN_{7–10}$-coated beads was suppressed by 53% after the expression of dominant-negative Rac ($P < 0.005$; Fig. 1 c). Focal complex formation was not reduced in cells expressing either dominant-negative Rho or a control vector containing the same promoter without GTPase DNA (Fig. 1 c). Together, these data indicate that $FN_{7–10}$-coated beads induce Rac-dependent focal complex formation.

To determine whether focal complex formation was selective for fibronectin receptors or extended to VN receptors, 6-μm-diam beads were coated with either $FN_{7–10}$, VN, or Con A and incubated on the lamella of NIH 3T3 fibroblasts for 1 h. Antibody labeling demonstrated that vinculin (Fig. 2 a) as well as paxillin (unpublished data) were recruited to midsize (6- or 3-μm diam) $FN_{7–10}$-coated beads ($P < 0.005$) as punctate focal complexes. However, vinculin did not accumulate around VN- or Con A–coated midsize beads (Fig. 2 a). Increasing or decreasing the ligand density on the beads by fivefold increased or decreased the percentage of beads with recruitment by ~18%, respectively, indicating a relatively modest concentration dependence that may be analogous to the change in cell attachment force with ligand concentration (Palecek et al., 1997). These results suggest that focal complex formation is specific for fibronectin receptors.

Analysis of $FN_{7–10}$-, VN-, and Con A–coated 1-μm-diam beads (Fig. 2, b and c) revealed that they did not cause vinculin accumulation. The inability of the 1-μm-diam beads to stimulate vinculin recruitment might indicate that a ligand-coated surface must be larger than the 0.1-μm^2 contact area of a bound 1-μm-diam bead (Galbraith and Sheetz, 1999; Suzuki et al., 2000) to stimulate focal complex formation. However, we also observed that clusters of 1-μm $FN_{7–10}$-coated beads induced recruitment (unpublished data), suggesting that the distance over which the contacts are spread and not the actual ECM contact area is important. These data may explain the ability of cells to grow if attachments to subthreshold contact areas are spread over a larger distance (Chen et al., 1997). Moreover, these findings suggest that larger cytoskeletal contractile forces may be generated at multiple, separated adhesive sites than at a similar number of adhesive sites that are located within a compact area.

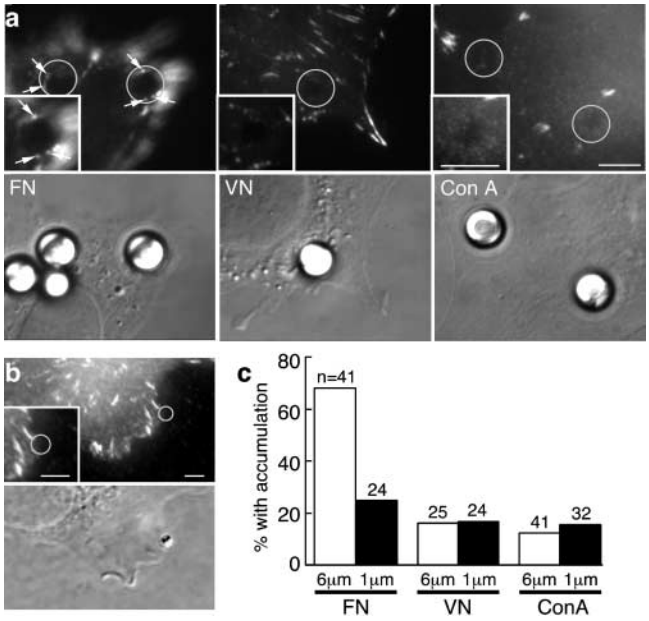

Figure 2. **Ligand surface area determines the ability to form focal complexes.** (a) Vinculin accumulates as punctate focal complexes around 6-μm $FN_{7–10}$-coated beads (inset, arrows), but it does not accumulate around VN- or Con A–coated beads. Top panels show immunofluorescence labeling of vinculin and bottom panels show DIC images. A circle on the fluorescence image indicates the position of the bead. Insets are higher magnification views of regions around the bead. Bars, 5 μm. (b) Focal complexes do not form around 1-μm $FN_{7–10}$-coated beads. Insets are higher magnification views of regions around the beads. Bars, 2 μm. (c) Only 6-μm $FN_{7–10}$-coated beads (FN) induce focal complexes ($P < 0.001$). VN- and Con A–coated beads do not induce focal complexes. Numbers indicate number of beads.

We further investigated the possible role of intracellular force on focal complex formation by incubating cells with 6-μm-diam $FN_{7–10}$-coated beads in the presence and absence of the specific myosin kinase inhibitor, ML-7, or the nonspecific protein kinase inhibitor, staurosporine. Both inhibitors significantly ($P < 0.001$) decreased vinculin accumulation around the 6-μm-diam $FN_{7–10}$-coated beads (45% of ML-7–treated beads had accumulation [$n = 56$] and 48% of staurosporine [$n = 23$]) compared with untreated controls (80% of untreated beads had accumulation [$n = 70$]). No significant differences were seen in these results when paxillin was used as an alternative marker for focal complexes. Thus, inhibition of myosin light chain kinase inhibits Rac-dependent focal complex formation.

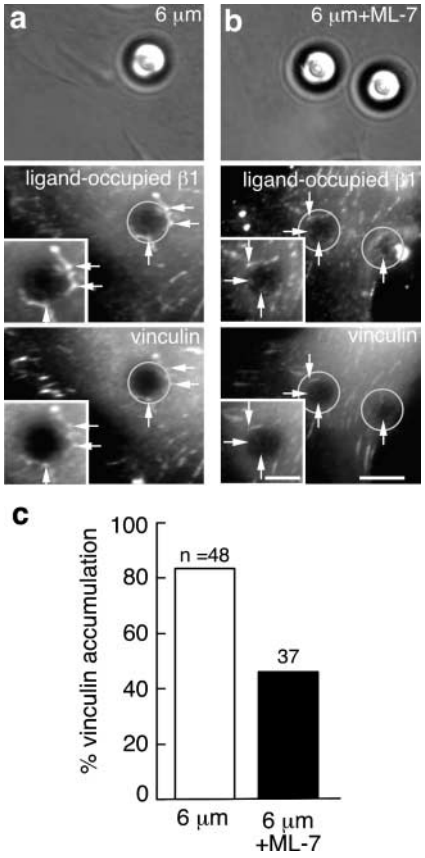

Figure 3. **Focal complex formation is dependent upon force.** (a) DIC and fluorescent images of ligand-occupied β1 integrin and vinculin when a 6-μm $FN_{7–10}$-coated bead adheres to a fibroblast lamella. Ligand-occupied β1 integrin and vinculin colocalize (arrows) in the focal complexes induced by the bead. A circle on the fluorescent images indicates the position of the bead. Insets are higher magnification views of regions around the bead. (b) DIC and fluorescent images of ligand-occupied β1 integrin and vinculin when a 6-μm $FN_{7–10}$-coated bead adheres to a fibroblast lamella in the presence of the myosin light chain kinase inhibitor, ML-7. Vinculin no longer colocalizes with most of the ligand-occupied β1 integrin around the bead (arrows). A circle on the fluorescent images indicates the position of the bead. Insets are higher magnification views of regions around the bead. Bars, 5 μm. (c) Vinculin colocalization with ligand-occupied β1 was significantly inhibited by the absence of force. Force was inhibited by the addition of 15 μM ML-7 ($P < 0.0005$) to 6-μm $FN_{7–10}$-coated beads.

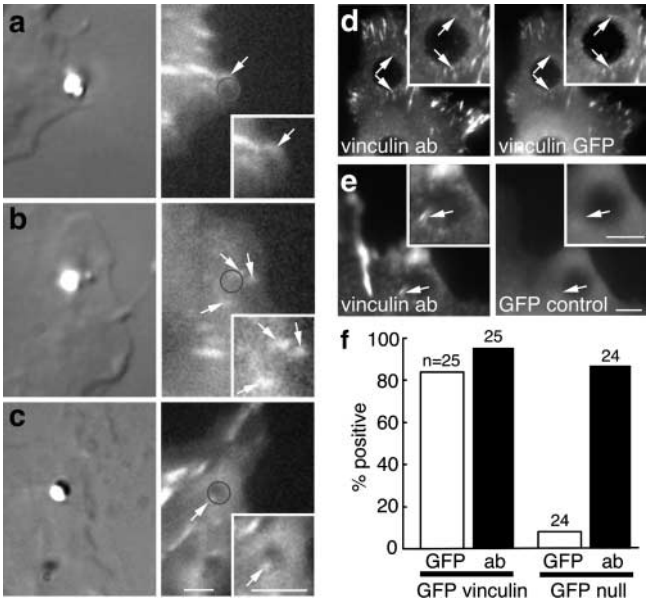

Figure 4. **Focal complexes are formed around small fibronectin-coated beads when external force is applied to the bead by an optical laser trap.** (a–c) DIC and fluorescence images of a 1-μm $FN_{7–10}$-coated bead initially constrained by an optical trap on the surface of a 3T3 fibroblast transfected with GFP-vinculin, illustrating the range of accumulation patterns of GFP-vinculin seen within 30 s around the surface of the bead as it escapes the force of the laser trap. (a) A focal complex formed and curved around a portion of the bead (arrow). (b) A group of focal complexes assembled at the bead perimeter (arrows). (c) A diffuse accumulation containing one or more punctate focal complexes surrounded the bead (arrow). A circle on the fluorescence images indicates the position of the bead. Insets are higher magnification views. Bars, 2 μm. (d) 3T3 fibroblasts were transfected with GFP-vinculin, incubated with 6-μm-diam $FN_{7–10}$-coated beads, and labeled with anti–vinculin antibody. GFP-vinculin and vinculin antibody show the same localization pattern around beads (arrows). Insets are higher magnification views of the area surrounding the bead. (e) 3T3 fibroblasts were transfected with a GFP control plasmid that contained the same promoter but lacked the vinculin insert. Cells were then incubated with 6-μm-diam $FN_{7–10}$-coated beads and labeled with anti–vinculin antibody. There was no specific GFP localization around the bead in the negative control (arrow). Insets are higher magnification views of the area surrounding the bead. Bars, 5 μm. (f) GFP localization was specific only in cells transfected with GFP-vinculin ($P < 0.001$). Numbers indicate number of beads.

Then, we tested whether actin–myosin contraction in the lamella could convert initial β1 integrin-FN adhesions into focal complexes. Immunofluorescence labeling indicates that there is an accumulation of ligand-occupied β1 integrin, part of a fibronectin receptor, around the $FN_{7–10}$-coated beads, and vinculin colocalizes with the ligand-occupied β1 integrin (Fig. 3 a, arrows, and Fig. 3 c). Similar colocalization was observed between vinculin and another marker for initial adhesions, talin (unpublished data). The addition of 15 μM ML-7 did not abolish the accumulation of ligand-occupied β1 integrin around the $FN_{7–10}$-coated beads (Fig. 3 b, arrows, and Fig. 3 c), but ML-7 did significantly inhibit ($P < 0.0005$) the colocalization of ligand-occupied β1 and vinculin (Fig. 3 b, arrows, and Fig. 3 c). A similar lack of colocalization (28% of beads examined had colocalization [$n = 32$], $P < 0.0001$) between ligand-occupied β1 and vinculin was seen around 1-μm-diam $FN_{7–10}$-coated beads. Together, these results indicate that initial β1 integrin–containing adhesions are formed with both small and midsize ligand-coated surfaces. However, internal cytoskeletal force causes these initial adhesions to develop into focal complexes on midsized ligand-coated surfaces, and an inhibitor of actin–myosin contractility can suppress this process.

External force induces focal complex formation

We investigated the hypothesis that externally applied force could induce the formation of focal complexes even when the ligand-coated surface was too small to trigger focal complex formation. An optical trap was used to constrain the movement of small, 1-μm-diam $FN_{7–10}$-coated beads on the actively moving lamellae of fibroblasts expressing low levels

of GFP-vinculin. In contrast to the lack of accumulation of vinculin around unrestrained 1-μm beads, vinculin accumulated near $FN_{7–10}$-coated beads placed on the lamella with the trap after 10–40 s of force restraint (76.5%, $n = 17$). The accumulation typically displayed one of the following patterns: (1) a focal complex formed that curved around a portion of the bead (Fig. 4 a); (2) a group of focal complexes assembled at the bead perimeter (Fig. 4 b); or (3) a diffuse accumulation of GFP-vinculin formed around the bead containing one or more punctate focal complexes (Fig. 4 c). In control experiments, GFP-vinculin showed a similar localization pattern to that of anti–vinculin antibody staining ($P < 0.001$), and the fluorescence obtained using the same GFP plasmid without the vinculin cDNA did not correlate with anti–vinculin antibody staining (Fig. 4, d–f). Thus, the force of the laser trap induced a specific accumulation of GFP-vinculin.

GFP-vinculin accumulation in response to external force often followed a typical sequence. GFP-vinculin was usually first detected as a diffuse aggregate on one side of the bead (Fig. 5, t = 16 s). As the aggregate condensed, usually on the side of the bead opposite the leading edge (Fig. 5, t = 48 s), the bead was pulled out of the laser trap. The ability of the bead to leave the restraining force of the laser trap indicates that the cell is pulling on the ECM-coated bead with a greater force than the trap is applying to hold the bead in place. This cytoskeletal pulling force is the same magnitude as the force used for migration (Galbraith and Sheetz, 1999). As the bead traveled rearward, the GFP-vinculin remained localized at the bead (Fig. 5, t = 88 s). However, as the bead traveled further into the lamella of the cell, the organization of GFP-vinculin became less punctate and surrounded the perimeter of the bead (Fig. 4, c and d; Fig. 5, t = 208 s). This concentrated localization around the bead did not appear to change over tens of minutes (unpublished data). These data demonstrate that external force applied from an optical trap can signal for vinculin to be recruited and focal complexes to form around a small FN-coated surface that could otherwise not produce focal complexes.

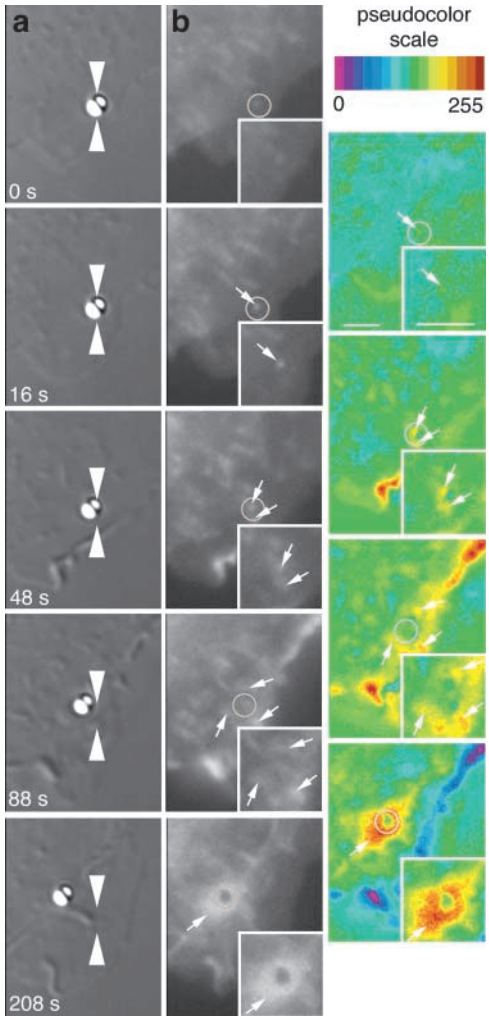

Figure 5. **Vinculin recruitment and focal complex formation follows a typical temporal and spatial pattern.** (a–c) Time series of GFP-vinculin accumulation around a 1-μm $FN_{7–10}$ coated bead initially constrained by an optical trap (t = 0 s). (a) Large arrowheads on DIC images mark the trap position. (b) Fluorescent images show that GFP-vinculin accumulation began as diffuse aggregates that approached the bead from the side of the cell opposite the leading edge (arrow, t = 48 s). GFP-vinculin condensed around the bead (arrow, t = 88, 128 s). GFP-vinculin remained localized at the bead, but it often loses its punctate localization and surrounds the bead (arrow, t = 208 s) as the bead travels inward on the lamella. (c) Pseudocolor images quantify the changes in fluorescence between adjacent images presented in b. Circles on the fluorescence and pseudocolor images indicate the position of the bead. Insets are higher magnification views. Bars, 2 μm.

Sustained vinculin recruitment indicates strengthened connections between fibronectin, integrin, and the cytoskeleton

To determine if the formation of focal complexes was indicative of the ability of an initial adhesion to exert migration force, we measured how the time course of GFP-vinculin accumulation correlated with the ability of the focal complex to exert force. Vinculin started to accumulate on the side of the bead near the leading edge just as the bead was about to escape the trap (Fig. 6, a and c, t = 27 s). The bead escaped the trap and vinculin was visualized as large punctate aggregates adjacent to the bead (Fig. 6, a and c, t = 54 s). However, in some cases, the vinculin localization suddenly dissipated ($n = 9$ of 32), and the bead returned to the laser trap (Fig. 6, a and c, t = 81 s) or increased in diffusion rate (not depicted). The loss of GFP-vinculin was not due to photobleaching. These results suggest that vinculin recruitment and focal complex formation is necessary for the cytoskeleton to exert force greater than the trap force on integrin receptors connected to the ECM-coated bead (i.e., to pull the bead out of the trap). Furthermore, the loss of vinculin binding at an adhesion site is accompanied by a decrease in the strength of the cytoskeletal connection to the adhesion.

If vinculin recruitment coincides with the strengthening of the connection between the cytoskeleton and the ECM at the focal complex, then reinforcement (strengthening) in proportion to ECM stiffness (Choquet et al., 1997) should correlate with vinculin recruitment. To test this hypothesis directly, we measured reinforcement of the connection between the cytoskeleton and the ECM, and monitored GFP-

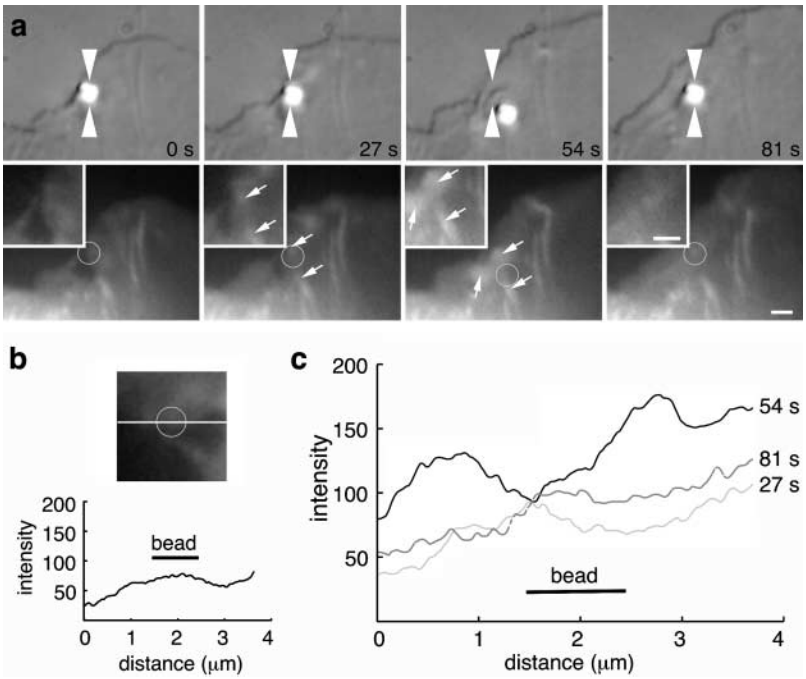

Figure 6. **Loss of vinculin binding to a focal complex is accompanied by a decrease in the strength of the cytoskeletal connection.** (a) Fluorescence and DIC images of a 1-μm ligand-coated bead constrained by an optical trap on a fibroblast transfected with GFP-vinculin. There is a small amount of GFP-vinculin as the bead begins to escape the trap (arrow, 27 s); there is a much larger recruitment around the bead when it is further from the trap center (arrow, 54 s), but the specific recruitment disappears as the bead returns to the trap center (81 s). Large arrowheads on DIC images mark the trap position. A circle on the fluorescence images indicates the position of the bead. Insets show higher magnification views of the bead. Arrows in the fluorescence insets indicate accumulation. Bars, 1 μm. (b) Immunofluorescence image is the inset from a at 0 s rotated 90° to the left. The circle indicates the bead position, and the horizontal line indicates the line used to measure fluorescence intensity. The fluorescence intensity is plotted as measured from left to right along the immunofluorescence image. The line labeled bead in the graph indicates the bead position. (c) Fluorescent line intensities of high magnification inserts as a function of position. There is a small increase of fluorescence, indicating a small increase in the amount of vinculin, on the side of the bead toward the leading edge of the cell at 27 s. At 54 s, there is an increase of fluorescence on both sides of the bead. At 81 s, the fluorescent intensity is similar to that at 27 s, but there is still a slight elevation underneath the bead.

vinculin recruitment to the same connections. In the reinforcement assay, a ligand-coated bead is placed on the cell and constrained with the optical trap (Fig. 7 a, t = 0 s). If the bead escapes the trap (Fig. 7 a, t = 5 s), then the trap is turned off, and the microscope stage is repositioned (Fig. 7 a, t = 5.5–14 s) so that the bead is within 0.5 μm of the trap center. When the connection between the bead and the cytoskeleton is reinforced, turning on the trap with the same power will not produce a significant displacement of the bead (less than the 100-nm displacement that can be attributed to rotation of the bead around an existing integrin connection (Choquet et al., 1997; Fig. 7 a, t = 14.4 s). If the connection between the bead and the cytoskeleton is not reinforced, then there is a large displacement of the

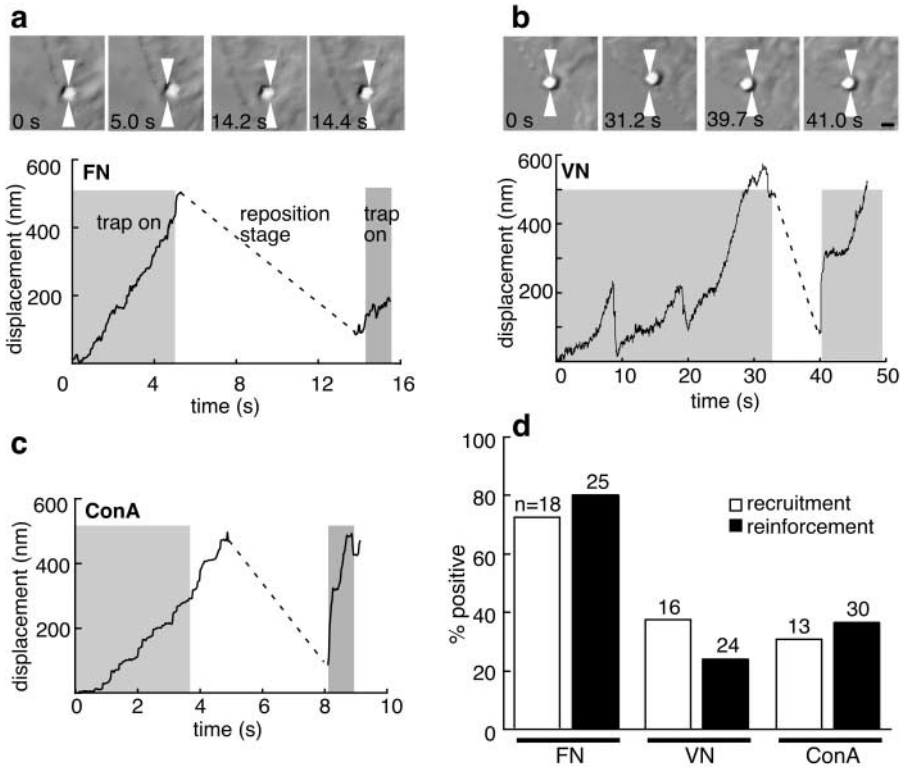

Figure 7. **Sustained vinculin recruitment indicates strengthened connections between fibronectin receptor and the cytoskeleton.** (a) FN–integrin–cytoskeletal connection is reinforced. FN_{7-10}-coated bead escapes from the optical trap; the trap is turned off, and the stage is repositioned. The trap is turned on again, and the bead does not return to the center of the trap. Note that the origin of the displacement trace has been repositioned during the stage repositioning so that all displacements appear to be positive. Arrowheads mark trap position. (b) VN–integrin–cytoskeletal connection is not reinforced. The VN-coated bead jumps to the center of the trap when trap is turned on again. Arrowheads mark trap position. Bar, 1 μm. (c) Con A–integrin–cytoskeletal connection is also not reinforced. (d) Only connections made between FN_{7-10}-coated beads, fibronectin receptors, and cytoskeleton showed significant vinculin recruitment ($P < 0.05$) and reinforcement ($P < 0.005$). Numbers indicate number of beads.

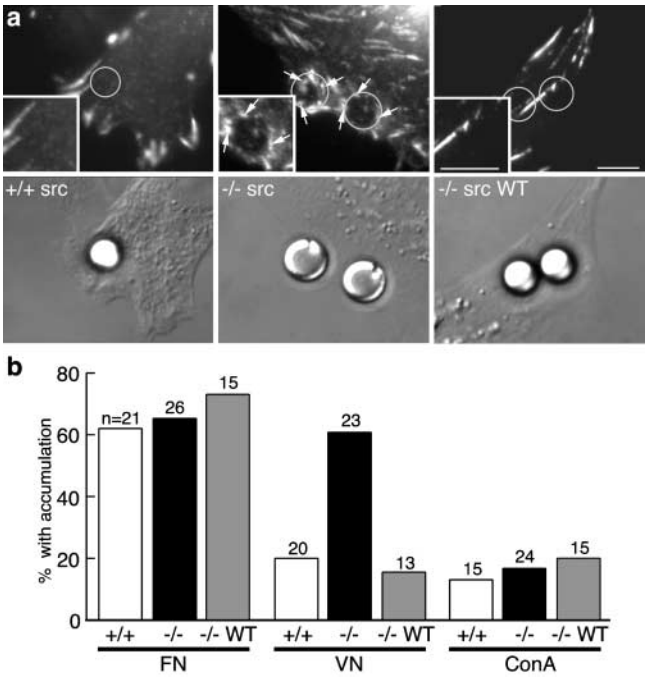

Figure 8. **c-Src regulates whether focal complexes form with VN receptors.** (a) Vinculin accumulates around 6-μm VN-coated beads on c-Src −/− cells (inset, arrows), but not around +/+ or −/− wild-type cells. A circle on the fluorescence images indicates the position of the bead. Insets show higher magnification views of the bead. Arrows in the fluorescence insets indicate accumulation. Bars, 5 μm. (b) Percentage of $FN_{7–10}$, VN, and Con A–coated 6-μm beads displaying vinculin recruitment on c-Src cells. Vinculin recruitment is sensitive to c-Src expression only with the VN-coated beads ($P < 0.05$). Numbers indicate number of beads.

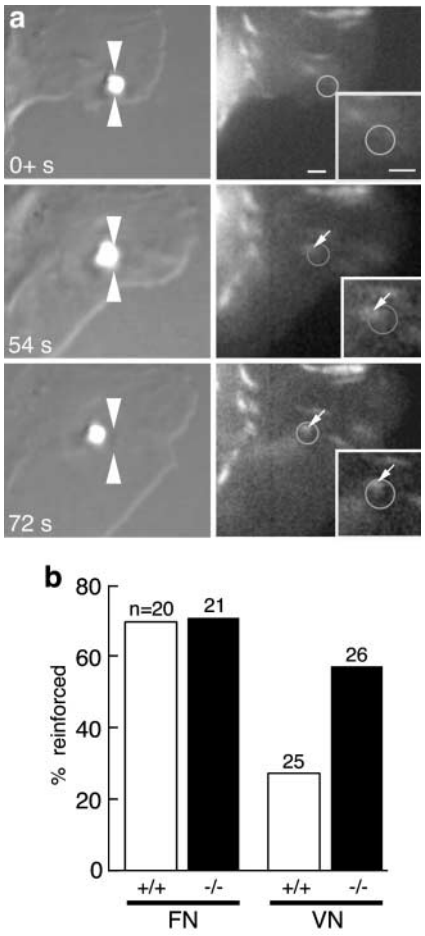

Figure 9. **Focal complexes formed with VN receptors recruit vinculin as they exert migration force.** (a) DIC and fluorescence images of a 1-μm VN-coated bead constrained by an optical trap on a c-Src −/− cell transfected with GFP-vinculin. The bead is in contact with the cell at 0^+ s. Vinculin was recruited to the side of the bead as it escaped the trap (arrow, 54 s). More vinculin is recruited to the periphery of the bead with time (72 s). A circle on the fluorescence images indicates the position of the bead. Arrows mark trap position in DIC images. Insets show higher magnification views of the area surrounding the bead. Bars, 1 μm. (b) Percentage of $FN_{7–10}$ or VN-coated beads showing reinforcement on c-Src −/− and c-Src +/+ cells. VN linkages only reinforce on c-Src −/− cells ($P < 0.05$). Numbers indicate number of beads.

bead (Fig. 7 b, t = 39.7 s, and Fig. 7 c, t = 8 s). Typically, $FN_{7–10}$ interactions were reinforced (80%; $P < 0.0005$), whereas VN (25%) and Con A (37%) interactions were not reinforced (Fig. 7 d). Reinforcement was not due to a difference in the binding of the beads to the cell because all beads bound similarly to the cell surface ($FN_{7–10}$, 86%, $n = 21$; VN, 71%, $n = 28$; Con A, 87%, $n = 23$), although VN-coated beads typically took slightly longer (30–60 s) to escape the laser trap. In separate experiments, the beads were restrained on the surface of 3T3 cells transfected with GFP-vinculin. On those cells, sustained GFP-vinculin recruitment was more likely to occur with $FN_{7–10}$ (72%; $P < 0.05$) than VN (37%) or Con A (Fig. 7 d; 31%). In a subset of experiments that was monitored for both recruitment and reinforcement, we found that 87% ($n = 15$) of the beads that exhibited reinforcement also exhibited recruitment of GFP-vinculin, irrespective of ligand coating. Importantly, we never observed vinculin accumulation in the absence of reinforcement. Thus, vinculin accumulation marks the strengthening of the connection between the ligand-coated bead and the cytoskeleton and the ability of the cell to exert force at focal complexes.

Focal complex formation at VN-coated surfaces occurs in the absence of c-Src

We also tested whether vinculin recruitment could indicate focal complex formation at integrin–ligand sites other than fibronectin receptors. Because VN receptor–cytoskeletal connections can become strengthened in the absence of c-Src (Felsenfeld et al., 1999), we tested whether focal complexes would form and sustain migration force in the absence of c-Src. VN-, $FN_{7–10}$-, and Con A–coated 6-μm beads were incubated on the surface of c-Src −/−, c-Src +/+, and c-Src −/− cells rescued with a wild-type c-Src (c-Src −/−WT). Immunofluorescence staining indicated that VN-coated beads induced recruitment of vinculin only in c-Src −/− cells (Fig. 8, a and b; $P < 0.005$). In contrast, $FN_{7–10}$-coated beads induced high levels of recruitment (62–73%), and Con A–coated beads induced low levels (13–20%) with all of the c-Src cell types (Fig. 8 b). Thus, in the absence of c-Src, both VN- and $FN_{7–10}$-coated surfaces induced punctate vinculin accumulations, and focal complex formation was extended to VN receptors.

To determine if there was a similar size and force dependence to the accumulation of vinculin under VN beads, we tested whether 1-μm-diam VN beads could cause vinculin accumulation on any of the c-Src cell types. Similar to the results obtained with 3T3 cells, vinculin did not accumulate around VN-, $FN_{7–10}$-, or Con A–coated 1-μm beads (unpublished data).

When we applied laser trap force on 1-μm VN-coated beads, there was an induction of GFP-vinculin accumulation that coincided with reinforcement in c-Src–deficient cells. Similar to the results obtained with NIH 3T3 cells, GFP-vinculin was recruited to one side of the bead as it escaped the trap (Fig. 9 a, t = 54 s), and a condensed GFP–vinculin complex traveled rearward with the bead on the lamella (Fig. 9 a, t = 77 s). The recruitment of GFP-vinculin to VN-coated beads was restricted to the c-Src–deficient cells (unpublished data). Although we consistently observed an accumulation of GFP-vinculin, the amount that was recruited in response to ligand-coated beads on c-Src −/− cells was typically not as large as that seen on either the c-Src +/+ or the 3T3 cells, suggesting a small decrease in vinculin recruitment in the absence of c-Src.

We also examined whether vinculin recruitment marked the strengthening of cytoskeleton–VN bead connections in the c-Src–deficient cells. The percentage of beads demonstrating vinculin recruitment (Fig. 8 b) correlated well with the percentage of beads showing reinforcement (Fig. 9 b). Furthermore, in a subset of experiments comparing reinforcement and GFP-vinculin recruitment, 76.9% of the cells (n = 13) that were reinforced also showed recruitment. These results demonstrate that in the absence of c-Src, both fibronectin and VN receptors can recruit vinculin to adhesive connections to form focal complexes and strengthen the connection between the cytoskeleton and the external ligand. Moreover, these results suggest that c-Src inhibits reinforcement of VN receptors by inhibiting the recruitment of vinculin.

Discussion

We have shown that initial adhesions between integrin receptors and ECM ligands gain the ability to exert significant migration forces on maturation into focal complexes. We have been able to induce the conversion of initial adhesions into focal complexes by the application of force to β1 integrin–FN connections from inside or outside the cell. Cell-generated contractile force in the lamellipodium is sufficient to form focal complexes around midsized beads coated with a fragment of fibronectin that is incapable of supporting focal adhesions. However, to form Rac-dependent focal complexes around beads that are too small to trigger focal complex assembly, external force that mimics stiffening of the ECM is needed. Focal complex formation, as marked by the recruitment of vinculin, is rapid (onset within 10–40 s), and loss of vinculin recruitment is accompanied by weakening of the force exerted at the adhesion, suggesting that vinculin binding stabilizes or strengthens the initial adhesion. The selectivity of vinculin recruitment and focal complex formation for the fibronectin receptor is extended to VN receptors in the absence of c-Src, suggesting that c-Src acts near the membrane to inhibit the recruitment of vinculin and/or stimulate the remodeling of VN receptor adhesion complexes. These results indicate that the application of force to initial adhesions induces the recruitment of vinculin and the formation of focal complexes that are capable of exerting migration force.

Our results indicate that the formation of a focal complex is the point at which force-induced cytoskeletal association of the integrin β1 with the cytoskeleton becomes strengthened. Thus, we propose that the phenomena of strengthening or reinforcement of initial ECM–integrin–cytoskeletal linkages (Choquet et al., 1997) is a consequence of the formation of focal complexes as indicated by the active recruitment of vinculin. This interpretation is supported by the ability of a β1-containing initial adhesion to exert force upon accumulation of vinculin, and the loss of force with the loss of vinculin accumulation. Evidence that the process is active and independent of recruitment of additional integrin to the initial adhesion comes from the lack of time dependence of adhesion strengthening (Choquet et al., 1997). If the process were passive and required additional integrin to strengthen initial adhesions, then the time required to recruit more freely diffusing unliganded integrin would be proportional to the strength of the applied force, but strengthening as well as the retrograde speed of particles are independent of the number of integrins recruited to the bead (Choquet et al., 1997). Thus, maturation of initial adhesions into focal complexes is an active process that provides a potential mechanism for early regulation of the strength of individual adhesion sites at localized regions of the advancing lamella.

The ligand and c-Src dependency of focal complex formation was independent of whether the complexes were induced by unconstrained midsize or by small ligand-coated beads that were optically trapped to apply force. One model that could explain why both methods produced similar accumulations of vinculin is that force is generated on midsized beads by local myosin-driven contraction acting on either side of the bead. In lamellipodial regions, the actin filament network undergoes a myosin-driven contraction (Svitkina et al., 1997) as it moves rearward (Evans, 1993). This model predicts that there is a minimum spacing (Svitkina et al., 1997) for contractile force generation between actin filaments in the network, and myosin contraction of filaments on either side of the midsize bead (>3-μm diam) can generate force, causing assembly of vinculin at the bead periphery. However, small beads (<2-μm diam) are too tiny to stimulate the recruitment of vinculin (Fig. 10 a). This is supported by the observation of a reduction in the percentage of midsize beads exhibiting Rac-dependent focal complexes marked by vinculin or paxillin by ∼45% in the presence of the specific myosin light chain kinase inhibitor, ML-7 (Fig. 3 c), or the nonspecific kinase inhibitor, staurosporine. The recruitment of vinculin to the midsize beads is an example of a type of inside-to-outside mechanical signal-inducing focal complexes (Fig. 10 b), whereas recruitment to optically trapped small beads is an example of a type of outside-to-inside mechanical signal inducing focal complex formation (Fig. 10 c). Therefore, we postulate that the formation of focal complexes and the recruitment of vinculin to both midsize beads and optically trapped small beads is

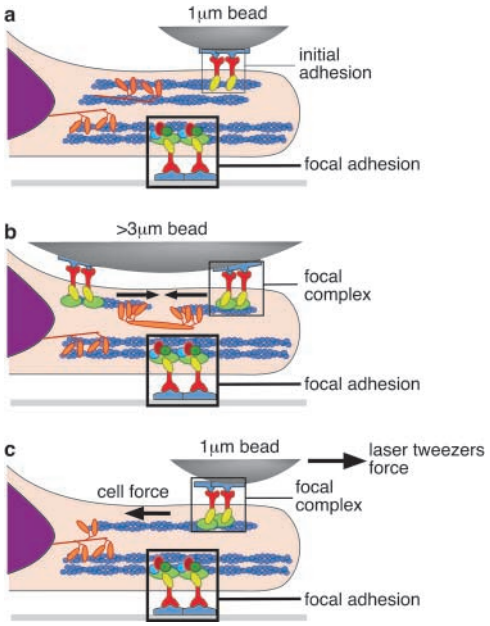

Figure 10. **Mechanical force determines the type of adhesive complexes formed as ligand-coated surfaces bind to integrin receptors.** (a) The initial adhesions between a small ligand-coated surface and integrin receptors produce an initial adhesion that moves rearward with retrograde actin flow. A focal adhesion can be formed against a larger ligand-coated surface that is physically restrained. More intracellular proteins are involved in the focal adhesion than the focal complex. (b) Midsized ligand-coated surfaces allow the cytoskeleton to contract mechanically, and they signal for the recruitment of proteins involved in focal complex formation. (c) Focal complexes can also be formed if mechanical force is applied externally by a laser trap.

dependent upon mechanical force, but independent of whether the force is applied from inside or outside the cell.

The transformation of the initial integrin–ECM adhesive contacts into focal complexes provides insight into how a cell regulates the amount of force exerted at adhesions. Focal complexes appear to be sites where the cell exerts more dynamic, but lower forces compared with forces exerted by focal adhesions. According to our reinforcement assay, as initial adhesions became focal complexes, they were capable of exerting a force >1 nN/μm^2, but <3 nN/μm^2. These forces are in good agreement with our previously measured traction force of 0.8–0.9 nN/μm^2 (Galbraith and Sheetz, 1997, 1999) in the lamella region. They are smaller than the forces reported for focal adhesions, which range from 4 to 5.5 nN/μm^2 (Galbraith and Sheetz, 1997; Balaban et al., 2001; Beningo et al., 2001), perhaps because a focal complex may have fewer structural components than a focal adhesion (Geiger et al., 2001). Thus, our data suggest that the initial adhesive complexes between FN receptors and ECM transduce cytoskeletal force into recruitment of vinculin and focal complex formation, and that the strength of focal complexes is less than that of focal adhesions. This early strengthening event from initial adhesions to focal complexes may then be followed by the Rho-dependent strengthening of focal complexes to focal adhesions (Riveline et al., 2001).

Although vinculin recruitment marks the strengthening of focal complexes, vinculin may not be the only protein responsible for strengthening. It is probable that several other proteins, including paxillin, act together as part of a strengthening complex. However, the role of any individual component may be difficult to discern because of compensation by other adhesion proteins in deficient cells (Volberg et al., 1995) as well as changes in kinase activity (Xu et al., 1998) and tyrosine phosphorylation levels (Xu et al., 1998) in deficient cells. Still, the strong correlation between reinforcement of focal complexes and the accumulation of vinculin suggests that vinculin has an essential role in strengthening the connections between integrin receptors and the cytoskeleton, and that the regulatory role of vinculin in force-dependent assembly of adhesive complexes is now of particular interest.

The correlation between the strengthening of initial fibronectin–receptor–cytoskeleton complexes and the accumulation of vinculin suggests that vinculin recruitment marks the development of these adhesive sites into focal complexes that are capable of exerting migration force. The speed of the accumulation, the local punctate accumulation, and ability of c-Src to inhibit focal complexes at VN integrin receptors indicates that focal complex formation is locally regulated. Local control provides the cell with a mechanism to modulate the timing and the location of force transmission to the ECM at individual adhesive contacts. The cell then has the capability to effectively regulate spreading and migration in response to force, which is consistent with the ability of substrate stiffness to guide migration (Mandeville et al., 1997; Lo et al., 2000).

Materials and methods

Cell culture and transfection

NIH 3T3 fibroblasts were grown in DME supplemented with 10% BCS, 2 mM L-glutamine, and 100 U/ml penicillin-streptomycin. For binding experiments with FN_{7-10}, the serum was replaced with 10% FBS, and for microscopy experiments, the DME in the binding media was replaced by DME with 25 mM Hepes and without phenol red. For binding experiments with VN, serum was replaced with 0.5% BSA. For all experiments, the cells were plated on silanized coverslips (Regen and Horwitz, 1992) coated with 40 μg/ml laminin. c-Src cell lines were grown in FN-binding media; the microscopy media and coverslip coatings were the same as those used for 3T3 cells.

Cells were transfected with GFP-vinculin with LipofectAMINE™ Plus for 1 h (Life Technologies). Cells with low levels of vinculin expression were used for live-cell imaging. Low levels of expression were chosen to yield good fluorescence signal-to-noise and healthy lamella during repeated exposure to the mercury arc lamp during the time course of the experiment.

Anti–human vinculin antibody was obtained from Sigma-Aldrich, and ligand-occupied β1 (9EG7) and anti–paxillin antibodies were obtained from BD Biosciences. Secondary antibodies were obtained from Jackson ImmunoResearch Laboratories.

The same method of transfection was used to induce cellular expression of VSV-tagged dominant-negative Rac or dominant-negative Rho. Expression of these plasmids was detected by immunostaining transfected cells with anti-VSV from Roche that were directly labeled with Alexa 565 from Molecular Probes, Inc. Cells chosen for analysis had comparable expression levels as judged by VSV fluorescence. Vinculin accumulation was detected by vinculin antibody directly labeled with Alexa 488. Control experiments indicated that these expression levels had a significant effect on the actin cytoskeleton as judged by Oregon green phalloidin labeling.

For myosin inhibition experiments, cells were preincubated with either 15 μM ML-7 or 50 nM staurosporine for 10 min before incubation with ligand-coated beads in the presence of the inhibitor. These concentrations were chosen from control experiments to produce comparable effects on the lamella f-actin.

Bead coating and static bead–binding assays

Beads (carboxylated polystyrene beads; Polysciences, Inc.) were coated with biotinylated FN_{7-10}, VN, or Con A according to the method described

previously (Felsenfeld et al., 1999). Coated beads were incubated with the cells for 1 h. Cells were washed, fixed, and immunofluorescently labeled according to the method described previously (Galbraith et al., 1998). Only beads on the flat lamella region of the cell were scored. Control experiments were performed to determine if the beads were internalized after 1 h of incubation. Cells were labeled for a surface receptor, which was not seen on the membrane above the beads on the lamella region; however, it was present above beads that attached to thicker regions of the cell body.

In additional control experiments to examine the effect of bead incubation time, only 20% fewer FN_{7-10}-coated beads were scored as positive ($n = 21$) for vinculin accumulation after 20 min. However, at 20 min, fewer beads bound to the surface of the cell due to the low ligand concentration; there were ~4–10 functional ligands on a small bead constrained in the laser trap (Felsenfeld, D.P., and M.P. Sheetz, personal communication). Because only beads that were that adhered to the flat lamella were scored, 1-h incubations were used to increase the number of events per experiment.

Optical gradient trap

An optical gradient trap similar to those described previously (Sterba and Sheetz, 1998) was constructed with the following modifications: a Tsunami laser (Spectra-Physics) was used as the trapping laser at 847 nm in continuous wavelength mode. To allow simultaneous visualization and recording of GFP and video-enhanced differential interference contrast (DIC) images while using the optical gradient trap, GFP was excited through the epi-illumination port on an inverted microscope (Axiovert 100; Carl Zeiss MicroImaging, Inc.), with the exciter of an Endow GFP Bandpass filter set and a dichroic mirror (model 496CDXT; Chroma Technology Corp.) that passed the laser light. The Endow GFP Bandpass emission filter was placed outside the microscope body in a Lambda-10 filter wheel (Sutter Instrument Co.) placed at the end of a Nikon multi-image module (see Fig. 2 of Sterba and Sheetz [1998] for placement of the image module). To obtain DIC images, the filter wheel was rotated to a position that contained a polarizer that was crossed with the DIC analyzer located above the microscope condenser. This imaging scheme allowed exact registration of the DIC and fluorescent images. Images were collected every 5–9 s with a Princeton Instruments MicroMAX camera (Roper Scientific), and a Newvicon camera (model VE-1000; DAGE-MTI, Inc.) was used in parallel to visualize and optically trap beads in real-time. The epifluorescence shutter, filter wheel, and camera were all controlled by custom software routines written using ISee (Inovision Corp.). Additional static incubation experiments were collected with MetaMorph® software (Universal Imaging Corp.).

The stiffness of the optical gradient trap was determined by measuring the displacement of the bead held in a trap while it was subjected to fluid force produced by moving the mechanical stage back and forth (Svoboda and Block, 1994). The average trap stiffness used in these experiments was 0.41 ± 0.07 pN/nm at a laser power of 65 mW. All beads were initially placed ~0.5 μm behind the leading edge of the lamella to ensure consistency.

Image processing and analysis

The nano-track cross-correlation routine within the ISee software was used to track the bead position during optical trap experiments. Control experiments indicated that this software had a tracking accuracy of 4–5 nm for the centroid of an immobilized 1-μm-diam particle (Felsenfeld, D.P., and M.P. Sheetz, personal communication).

To determine if the fluorescent vinculin accumulation was related to bead position, the DIC and fluorescent images were superimposed, and only fluorescent accumulations that were associated with the bead perimeter as either a small tangential mark or a mark that followed the contour were scored as positive accumulations. Control experiments were performed to ensure scoring consistency. Random blind scoring was performed of a significant portion of the original data. Simulations were performed with the experiments in which the cells were labeled for both ligand-activated β1 integrin and vinculin; in these controls the observer did not know the bead position from the DIC images, but was able to consistently identify the bead position in both of the fluorescent images. In addition, rescoring of all of the live-cell GFP-vinculin accumulation experiments by a blinded observer yielded consistent results. To determine if the vinculin accumulation shown by GFP-vinculin correlated with the accumulation detected by antibody labeling, cells were transfected with GFP-vinculin, incubated with ligand-coated beads as described above, and then fixed and immunofluorescently labeled for vinculin. As an additional control for the specificity of GFP-vinculin, cells were transfected with a GFP-null plasmid containing the same promoter, incubated with ligand-coated beads, and then immunofluorescently labeled for vinculin.

Adobe Photoshop® was used to determine the difference and pseudocolor fluorescence intensity between series of images. Images were subtracted using the Apply Image function. The minimum and the maximum pixel value of each resultant image was determined, and the entire collection of resultant images was scaled by stretching the image to the collection minimum and the collection maximum. The images were then converted to indexed color and mapped onto the color table defined in Fig. 5.

All images compared for intensity were contrast-enhanced by stretching each image to the collection minimum and the collection maximum. A line scan was then performed in the center of the high magnification inset image (Fig. 6) using NIH Image 1.62 software (available at http://rsb.info.nih.gov/nih-image). The intensity of the zero time point is presented and the intensity profiles obtained from all subsequent time points were offset by this baseline level.

The contact area between the bead and the cell surface was calculated by estimating the distance that the bead was displaced into the surface of the lamella during initial placement by the trap. This distance was equated to the displacement of the centroid of either the white or the black half of the DIC image of the bead (not depicted). The contact area is the surface area of a segment of a sphere of this height. The height was also measured from scanning electron microscopy micrographs of beads that had been placed on the surface of a cell by a laser trap, and this value was slightly lower. The values obtained from these two different methods ranged from 0.05 to 0.17 μm^2.

All experiments were performed at least in triplicate. Statistical analysis was performed using Prism software (GraphPad Software, Inc.). χ^2 tests were performed for statistics, and Fisher exact tests were performed when contingency tables were subdivided for multiple comparisons.

We thank S. Bershadsky, M. Elbaum, and B. Geiger (Weizmann Institute, Rehovot, Israel) for stimulating discussions and GFP-vinculin, D. Felsenfeld, J. Galbraith, M. Larsen, and K. Clark for comments and suggestions, P. Schwartzberg (National Human Genome Research Institute, NIH, Bethesda, MD) and P. Soriano (Fred Hutchinson Cancer Research Center, Seattle, WA) for c-Src–deficient cells, H. Erickson (Duke University, Durham, NC) for FN_{7-10}, K. Matsumoto (National Institute of Dental and Craniofacial Research, NIH) for the dominant-negative Rac and Rho plasmids, and J.S. Gutkind (National Institute of Dental and Craniofacial Research, NIH) for the Rac and Rho cDNA (Coso et al., 1995).

This work was supported by Office of Naval Research grant (N00014-97-0911) and National Institutes of Health grant (GM 36277-15) to M.P. Sheetz, and the National Institute of Dental and Craniofacial Research.

Submitted: 29 April 2002
Revised: 21 October 2002
Accepted: 21 October 2002

References

Balaban, N.Q., U.S. Schwarz, D. Riveline, P. Goichberg, G. Tzur, I. Sabanay, D. Mahalu, S. Safran, A. Bershadsky, L. Addadi, and B. Geiger. 2001. Force and focal adhesion assembly: a close relationship studied using elastic micropatterned substrates. *Nat. Cell Biol.* 3:466–472.

Beningo, K.A., M. Dembo, I. Kaverina, J.V. Small, and Y.L. Wang. 2001. Nascent focal adhesions are responsible for the generation of strong propulsive forces in migrating fibroblasts. *J. Cell Biol.* 153:881–888.

Bloom, L., K.C. Ingham, and R.O. Hynes. 1999. Fibronectin regulates assembly of actin filaments and focal contacts in cultured cells via the heparin-binding site in repeat III13. *Mol. Biol. Cell.* 10:1521–1536.

Chen, C.S., M. Mrksich, S. Huang, G.M. Whitesides, and D.E. Ingber. 1997. Geometric control of cell life and death. *Science.* 276:1425–1428.

Choquet, D., D.P. Felsenfeld, and M.P. Sheetz. 1997. Extracellular matrix rigidity causes strengthening of integrin-cytoskeleton linkages. *Cell.* 88:39–48.

Coso, O.A., M. Chiariello, J.C. Yu, H. Teramoto, P. Crespo, N. Xu, T. Miki, and J.S. Gutkind. 1995. The small GTP-binding proteins Rac1 and Cdc42 regulate the activity of the JNK/SAPK signaling pathway. *Cell.* 81:1137–1146.

DePasquale, J.A., and C.S. Izzard. 1987. Evidence for an actin-containing cytoplasmic precursor of the focal contact and the timing of incorporation of vinculin at the focal contact. *J. Cell Biol.* 105:2803–2809.

Evans, E. 1993. New physical concepts for cell amoeboid motion. *Biophys. J.* 64: 1306–1322.

Felsenfeld, D.P., P.L. Schwartzberg, A. Venegas, R. Tse, and M.P. Sheetz. 1999. Selective regulation of integrin–cytoskeleton interactions by the tyrosine kinase Src. *Nat. Cell Biol.* 1:200–206.

Galbraith, C.G., and M.P. Sheetz. 1997. A micromachined device provides a new bend on fibroblast traction forces. *Proc. Natl. Acad. Sci. USA.* 94:9114–9118.

Galbraith, C.G., and M.P. Sheetz. 1999. Keratocytes pull with similar forces on their dorsal and ventral surfaces. *J. Cell Biol.* 147:1313–1324.

Galbraith, C.G., R. Skalak, and S. Chien. 1998. Shear stress induces spatial reorganization of the endothelial cell cytoskeleton. *Cell Motil. Cytoskeleton.* 40: 317–330.

Geiger, B., and A. Bershadsky. 2001. Assembly and mechanosensory function of focal contacts. *Curr. Opin. Cell Biol.* 13:584–592.

Geiger, B., A. Bershadsky, R. Pankov, and K.M. Yamada. 2001. Transmembrane crosstalk between the extracellular matrix and the cytoskeleton. *Nat. Rev. Mol. Cell Biol.* 2:793–805.

Grinnell, F., and B. Geiger. 1986. Interaction of fibronectin-coated beads with attached and spread fibroblasts. Binding, phagocytosis, and cytoskeletal reorganization. *Exp. Cell Res.* 162:449–461.

Izzard, C.S. 1988. A precursor of the focal contact in cultured fibroblasts. *Cell Motil. Cytoskeleton.* 10:137–142.

Izzard, C.S., R. Radinsky, and L.A. Culp. 1986. Substratum contacts and cytoskeletal reorganization of BALB/c 3T3 cells on a cell-binding fragment and heparin-binding fragments of plasma fibronectin. *Exp. Cell Res.* 165:320–336.

Kraynov, V.S., C. Chamberlain, G.M. Bokoch, M.A. Schwartz, S. Slabaugh, and K.M. Hahn. 2000. Localized Rac activation dynamics visualized in living cells. *Science.* 290:333–337.

Lauffenburger, D.A., and A.F. Horwitz. 1996. Cell migration: a physically integrated molecular process. *Cell.* 84:359–369.

Lee, J., M. Leonard, T. Oliver, A. Ishihara, and K. Jacobson. 1994. Traction forces generated by locomoting keratocytes. *J. Cell Biol.* 127:1957–1964.

Lo, C.M., H.B. Wang, M. Dembo, and Y.L. Wang. 2000. Cell movement is guided by the rigidity of the substrate. *Biophys. J.* 79:144–152.

Mandeville, J.T., M.A. Lawson, and F.R. Maxfield. 1997. Dynamic imaging of neutrophil migration in three dimensions: mechanical interactions between cells and matrix. *J. Leukoc. Biol.* 61:188–200.

Miyamoto, S., S.K. Akiyama, and K.M. Yamada. 1995. Synergistic roles for receptor occupancy and aggregation in integrin transmembrane function. *Science.* 267:883–885.

Nobes, C.D., and A. Hall. 1995. Rho, rac, and cdc42 GTPases regulate the assembly of multimolecular focal complexes associated with actin stress fibers, lamellipodia, and filopodia. *Cell.* 81:53–62.

Palecek, S.P., J.C. Loftus, M.H. Ginsberg, D.A. Lauffenburger, and A.F. Horwitz. 1997. Integrin-ligand binding properties govern cell migration speed through cell-substratum adhesiveness. *Nature.* 385:537–540.

Pelham, R.J., and Y. Wang. 1999. High resolution detection of mechanical forces exerted by locomoting fibroblasts on the substrate. *Mol. Biol. Cell.* 10:935–945.

Regen, C.M., and A.F. Horwitz. 1992. Dynamics of beta 1 integrin-mediated adhesive contacts in motile fibroblasts. *J. Cell Biol.* 119:1347–1359.

Riveline, D., E. Zamir, N.Q. Balaban, U.S. Schwarz, T. Ishizaki, S. Narumiya, Z. Kam, B. Geiger, and A.D. Bershadsky. 2001. Focal contacts as mechanosensors: externally applied local mechanical force induces growth of focal contacts by an mDia1-dependent and ROCK-independent mechanism. *J. Cell Biol*. 153:1175–1186.

Rottner, K., A. Hall, and J.V. Small. 1999. Interplay between Rac and Rho in the control of substrate contact dynamics. *Curr. Biol.* 9:640–648.

Saoncella, S., F. Echtermeyer, F. Denhez, J.K. Nowlen, D.F. Mosher, S.D. Robinson, R.O. Hynes, and P.F. Goetinck. 1999. Syndecan-4 signals cooperatively with integrins in a Rho-dependent manner in the assembly of focal adhesions and actin stress fibers. *Proc. Natl. Acad. Sci. USA.* 96:2805–2810.

Sastry, S.K., and K. Burridge. 2000. Focal adhesions: a nexus for intracellular signaling and cytoskeletal dynamics. *Exp. Cell Res.* 261:25–36.

Sheetz, M.P., D.P. Felsenfeld, and C.G. Galbraith. 1998. Cell migration: regulation of force on extracellular-matrix-integrin complexes. *Trends Cell Biol.* 8:51–54.

Sterba, R.E., and M.P. Sheetz. 1998. Basic laser tweezers. *Methods Cell Biol.* 55:29–41.

Suzuki, K., R.E. Sterba, and M.P. Sheetz. 2000. Outer membrane monolayer domains from two-dimensional surface scanning resistance measurements. *Biophys. J.* 79:448–459.

Svitkina, T.M., A.B. Verkhovsky, K.M. McQuade, and G.G. Borisy. 1997. Analysis of the actin-myosin II system in fish epidermal keratocytes: mechanism of cell body translocation. *J. Cell Biol.* 139:397–415.

Svoboda, K., and S.M. Block. 1994. Biological applications of optical forces. *Annu. Rev. Biophys. Biomol. Struct.* 23:247–285.

Volberg, T., B. Geiger, Z. Kam, R. Pankov, I. Simcha, H. Sabanay, J.L. Coll, E. Adamson, and A. Ben-Ze'ev. 1995. Focal adhesion formation by F9 embryonal carcinoma cells after vinculin gene disruption. *J. Cell Sci.* 108:2253–2260.

Vuori, K., and E. Ruoslahti. 1999. Connections count in cell migration. *Nat. Cell Biol.* 1:E85–E87.

Woods, A., J.R. Couchman, S. Johansson, and M. Hook. 1986. Adhesion and cytoskeletal organisation of fibroblasts in response to fibronectin fragments. *EMBO J.* 5:665–670.

Xu, W., H. Baribault, and E.D. Adamson. 1998. Vinculin knockout results in heart and brain defects during embryonic development. *Development.* 125: 327–337.

Zamir, E., M. Katz, Y. Posen, N. Erez, K.M. Yamada, B.Z. Katz, S. Lin, D.C. Lin, A. Bershadsky, Z. Kam, and B. Geiger. 2000. Dynamics and segregation of cell-matrix adhesions in cultured fibroblasts. *Nat. Cell Biol.* 2:191–196.